AD NUMBER
AD910079
LIMITATION CHANGES
TO: **Approved for public release; distribution is unlimited.**
FROM: **Distribution authorized to U.S. Gov't. agencies only; Test and Evaluation; 11 APR 1973. Other requests shall be referred to Naval Underwater Systems Center, Newport, RI 02840.**
AUTHORITY
UNSC ltr, 23 Aug 1974

NUSC Technical Report 4322

Electromagnetic Surface Currents Induced By a Magnetic Dipole Source on Infinite Perfectly - Conducting Surfaces In the Presence of an Air-Ocean Interface.

Donald M. Bolle
Weapons Department

11 April 1973

NAVAL UNDERWATER SYSTEMS CENTER
Newport Laboratory

NUSC-TR-4322

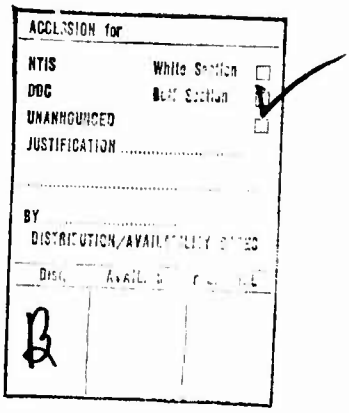

ADMINISTRATIVE INFORMATION

This investigation was performed as part of an exploratory development program for active electromagnetic detectors under Task Assignment No. ORD-541-451/091-1/UF17-351-501, Principal Investigator, Dr. Donald M. Bolle (Code PA1).

The Technical Reviewer for this report was Mr. Edward J. Hilliard, Jr. (Code SB11).

REVIEWED AND APPROVED: 11 April 1973

C. A. Spero, Jr.
Systems Development Director

Inquiries concerning this report may be addressed to the author at the Newport Laboratory, Naval Underwater Systems Center, Newport, Rhode Island 02840.

ABSTRACT

The electromagnetic surface currents induced by a magnetic dipole on infinite perfectly conducting surfaces in the presence of a sea-air interface, as well as in a homogeneous ocean environment, are obtained. The method used is that of images where the approximation of a -1 reflection coefficient at the sea-air interface may be justified and used. Computer programs and results which yield a clear insight into the sphere of influence of the magnetic dipole in such an environment when displayed graphically are given.

REVERSE BLANK

TABLE OF CONTENTS

LIST OF ILLUSTRATIONS

LIST OF SYMBOLS

$\underline{E}_p^i$	Electric Field Intensity of the Magnetic Dipole Source
$\underline{E}_T$	Total Electric Field Intensity
(r, θ, ϕ)	Spherical Coordinates
ω	Radian Frequency
μ	Permeability
ϵ	Permittivity
$(\underline{a}_r, \underline{a}_\theta, \underline{a}_\phi)$	Spherical Unit Vectors
E_o	Magnitude of the Incident Dipole Electric Field Intensity
N	Number of Turns on Dipole Source Coil
k	Propagation Factor
δ	Skin Depth
σ	Conductivity
(H_r, H_θ)	Components of the Magnetic Field Intensity
H_o	Magnitude of the Dipole Magnetic Field Intensity
(x', y', z')	Rectangular Coordinate System Centered on the Dipole
(θ_s, ϕ_s)	Orientation Angles for the Magnetic Dipole with respect to the (x, y, z) Coordinate System
(x, y, z)	Rectangular Coordinate System Centered with Scatterer
$\underline{J}$	Surface Current Density
$\underline{n}$	Surface Normal Unit Vector

LIST OF SYMBOLS (Cont'd)

$(\underline{a}_x, \underline{a}_y, \underline{a}_z)$	Cartesian Unit Vectors
ρ	Reflection Coefficient
m	Dipole Moment
(m_x, m_y, m_z)	Dipole Moment Components
d	Distance from Dipole to Conducting Plane
h	Depth of Dipole below Ocean-Air Interface
b	Baseline between Dipole Source and Detector

ELECTROMAGNETIC SURFACE CURRENTS INDUCED BY A MAGNETIC DIPOLE SOURCE ON INFINITE PERFECTLY CONDUCTING SURFACES IN THE PRESENCE OF AN AIR-OCEAN INTERFACE

INTRODUCTION

In the first part of this report, the electromagnetic surface current induced on a perfectly conducting infinite flat plate in a conducting medium for a magnetic dipole source is obtained. These results will allow the introduction of the effect of the sea-air interface in the second part of the report. The analysis employs the method of images.

The results will serve to illustrate the extent of the dipole influence when immersed in a conducting fluid, and thus, evaluate the effectiveness of the magnetic dipole as a detector in the ocean.

THEORY

INDUCED CURRENT ON INFINITE FLAT PLATES IN A LOSSY ENVIRONMENT: MAGNETIC DIPOLE EXCITATION

The electric field due to a magnetic dipole source is given by

$$\underline{E}_p^i/E_o = -j\left[(kr)^{-2} + j(kr)^{-1}\right] e^{-jkr} \sin\theta\, \underline{a}_\phi . \tag{1}$$

Thus the total field at P due to source and image is

$$\underline{E}_T/E_o = -j\left\{\left[(kr_1)^{-2} + j(kr_1)^{-1}\right] e^{-jkr_1} \sin\theta_1 - \left[(kr_2)^{-2} + j(kr_2)^{-1}\right] e^{-jkr_2} \sin\theta_2\right\} \underline{a}_\phi \tag{2}$$

where

$$E_o = \omega\mu NIdAk^2/4\pi = \omega\mu k^2 |\underline{m}|/4\pi . \tag{3}$$

NIdA is the magnitude of the magnetic dipole moment; N is the number of turns on the loop. Also

$$k = (1 - j)/\delta \tag{4}$$

$$\delta = (2/\omega\mu\sigma)^{1/2}. \tag{5}$$

Figure 1 illustrates the geometry considered, while figure 2 shows the solution using the method of images. Appendix A represents the computer program used.

The analysis is expanded to include the case where the dipole orientation with respect to the normal to the conducting plate is arbitrary and the approach to the plate may be at any angle θ_p. The following results pertain to the two cases: a magnetic dipole source normal to the path, and a magnetic dipole source in the direction of the path. For both cases, the current pattern induced on the conducting plate and the signal induced in the detector coil will be calculated. Figure 3 illustrates the generalized geometry, while figure 4 illustrates the image theory solution for the second case when $\phi_p = \pi/2$.

A general analysis which can handle all possible cases will be used, where the dipole source is given arbitrary orientation in space and the resultant field at any point in the same half space is obtained. A particular calculation will thus need to have the dipole orientation and location, as well as the detector location and orientation with respect to the dipole source, specified. A path for the dipole source-detector combination will be specified through controlling successive dipole source-detector locations along a linear path or along any general curve. In this study primary interest lies in obtaining the induced surface currents on the conducting plane at $y = -d$.

Since the dipole field components are given by

$$H_r/H_o = 2\left[(kr)^{-3} + j(kr)^{-2}\right] e^{-jkr} \cos\theta \tag{6}$$

$$H_\theta/H_o = \left[(kr)^{-3} + j(kr)^{-2} - (kr)^{-1}\right] e^{-jkr} \sin\theta \tag{7}$$

$$E_\phi/H_o = -j(\omega\mu/k)\left[(kr)^{-2} + j(kr)^{-1}\right] e^{-jkr} \sin\theta \tag{8}$$

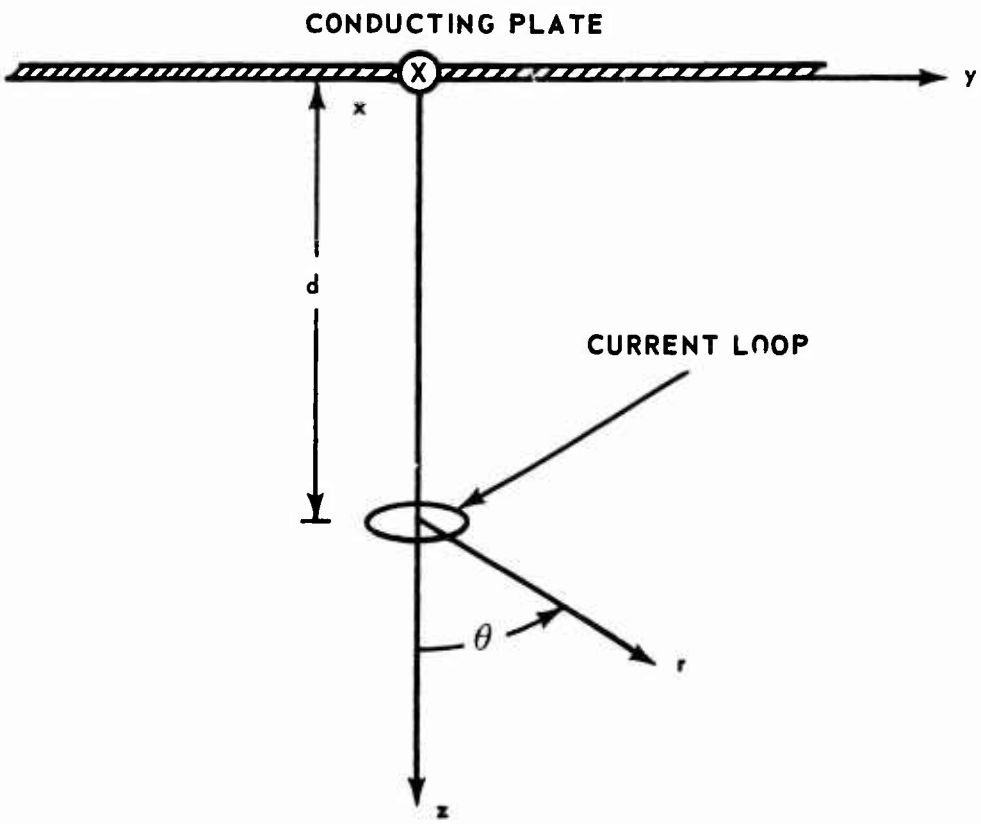

Figure 1. Problem Geometry

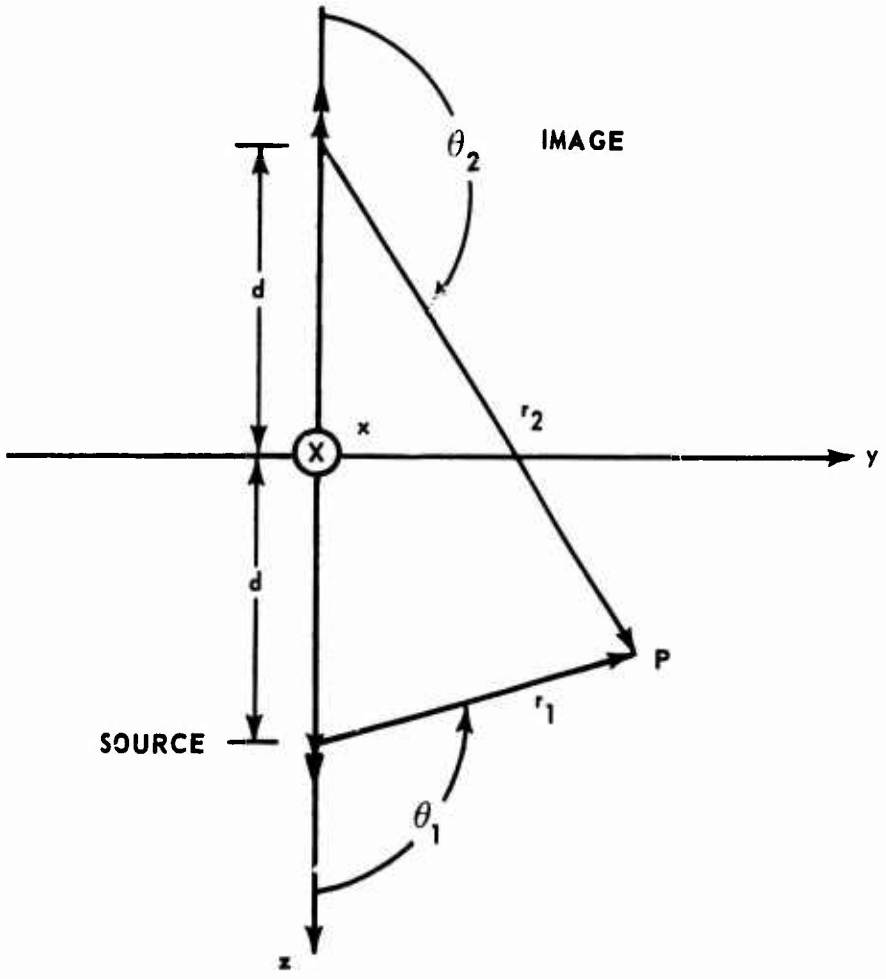

Figure 2. Image Solution

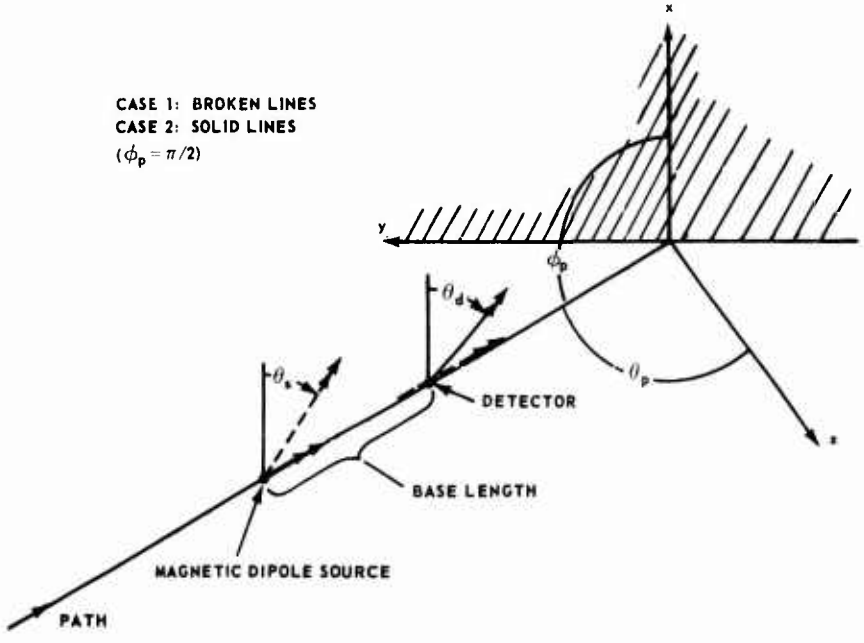

Figure 3. Generalized Geometry

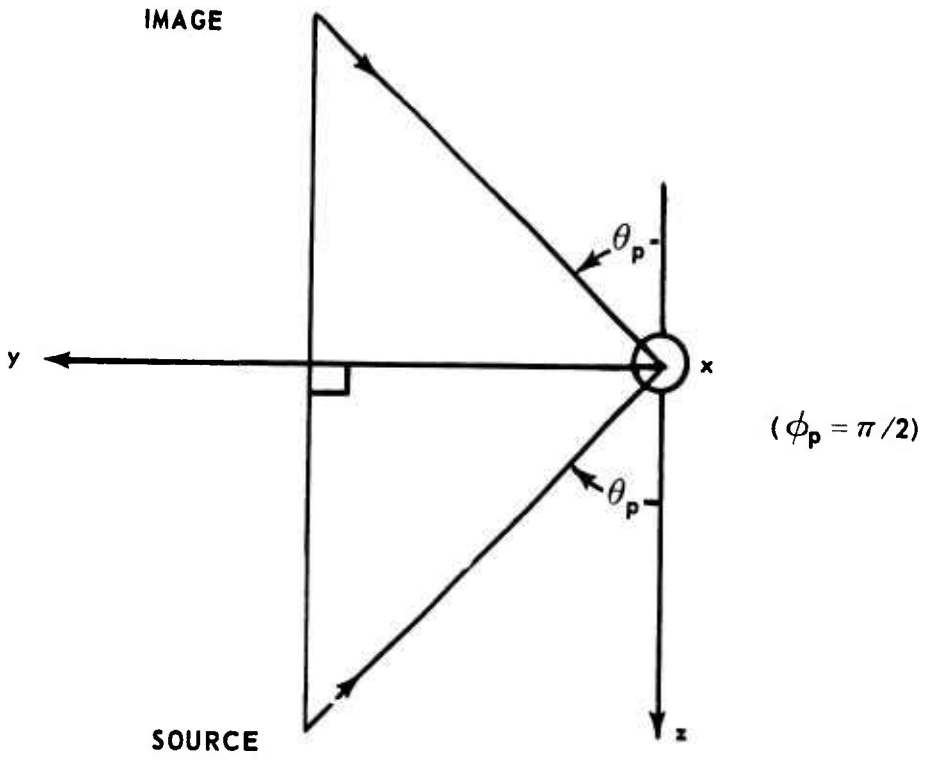

Figure 4. Image Solution (Case 2)

where

$$H_o = NIdAk^3/4\pi \tag{9}$$

and

$$NIdA = \text{magnitude of magnetic dipole moments,} \tag{10}$$

in terms of a local spherical coordinate system, this system must be related to the rectangular coordinate system which will describe the various bounding surfaces. The magnetic dipole source will, therefore, be taken to be oriented with angles θ_s, ϕ_s with respect to the rectangular system x, y, z, with the z axis coincident with $\theta_s = 0$ and the x axis coincident with $\phi_s = 0$. The perfectly conducting plane is taken to be the plane y = -d. Figure 5 illustrates this general situation.

Consider the point (x', y', z') which, in the local dipole spherical coordinate system, is the point (r, θ, ϕ); then the relationship between the two coordinate systems is given by

$$r = \left[x'^2 + y'^2 + z'^2\right]^{1/2} \tag{11}$$

$$\sin\theta = \left(x'^2 + y'^2\right)^{1/2}/r \tag{12}$$

$$\cos\theta = z'/r \tag{13}$$

where

$$x' = x\cos\phi_s + y\sin\phi_s \tag{14}$$

$$y' = \left(-x\sin\phi_s + y\cos\phi_s\right)\cos\theta_s - z\sin\theta_s \tag{15}$$

$$z' = \left(-x\sin\phi_s + y\cos\phi_s\right)\sin\theta_s + z\cos\theta_s . \tag{16}$$

Thus, given the location (x, y, z) at which the dipole field needs to be evaluated and the angles (θ_s, ϕ_s) giving the direction of the dipoles, the field components can be calculated using (14) through (16) in sequence with (11) through (13).

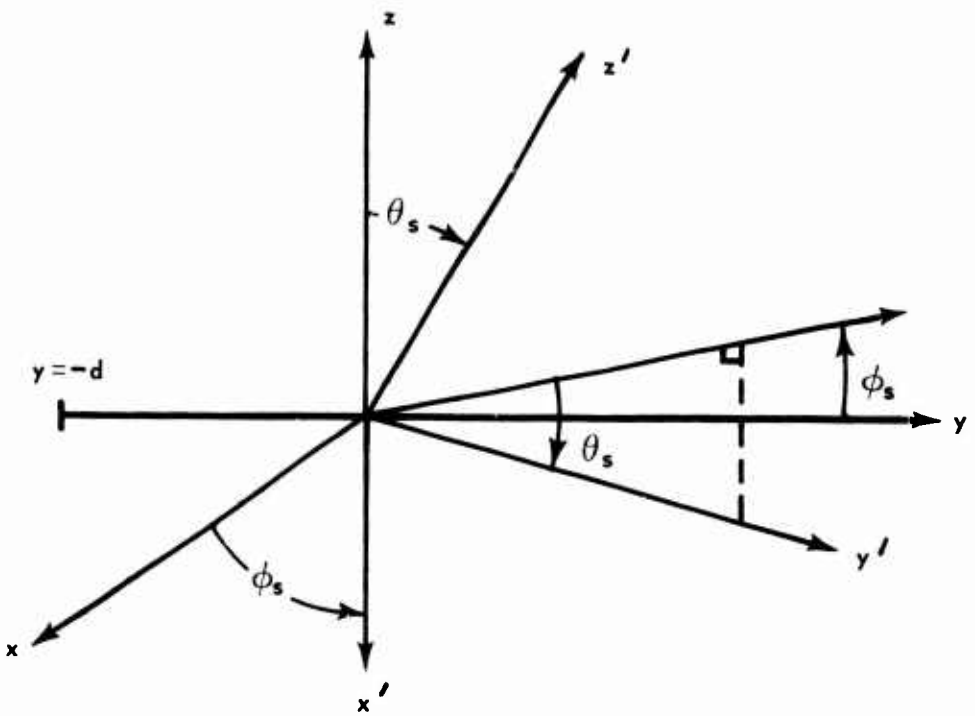

Figure 5. Dipole Coordinate Systems

In this case, because only infinite flat conducting planes are considered, the induced surface current is given by

$$\underline{J} = 2\underline{n} \times \underline{H}_s\Big|_{y=-d} \tag{17}$$

which is obtained from either physical optics or the theory of images, as these two approaches are fully equivalent in this situation. This can be rewritten as

$$\underline{J} = 2\underline{a}_y \times \underline{H}\Big|_{y=-d} = 2\underline{a}_y \times \left(H_r\underline{a}_r + H_\theta\underline{a}_\theta\right)\Big|_{y=-d} \tag{18}$$

and the relationship between the unit vectors in the local dipole spherical system and the rectangular coordinate system must be established. This is

$$\begin{aligned}\underline{a}_r = {} & \underline{a}_x\left[\cos\phi_s \sin\theta\cos\phi - \sin\phi_s\cos\theta_s\sin\theta\sin\phi - \sin\phi_s\sin\theta_s\cos\theta\right] \\ & + \underline{a}_y\left[\sin\phi_s\sin\theta\cos\phi + \cos\phi_s\cos\theta_s\sin\theta\sin\phi + \sin\theta_s\cos\phi_s\cos\theta\right] \\ & + \underline{a}_z\left[-\sin\theta_s\sin\theta\sin\phi + \cos\theta_s\cos\theta\right]\end{aligned} \tag{19}$$

$$\begin{aligned}\underline{a}_\theta = {} & \underline{a}_x\left[\cos\phi_s\cos\theta\cos\phi - \sin\phi_s\cos\theta_s\cos\theta\sin\phi + \sin\theta_s\sin\phi_s\sin\theta\right] \\ & + \underline{a}_y\left[\sin\phi_s\cos\theta\cos\phi + \cos\theta_s\cos\phi_s\cos\theta\sin\phi - \sin\theta_s\cos\phi_s\sin\theta\right] \\ & + \underline{a}_z\left[-\sin\theta_s\cos\theta\sin\phi - \cos\theta_s\sin\theta\right].\end{aligned} \tag{20}$$

The two components of the surface current density then take the form

$$\begin{aligned}J_x = \Big\{ & 2H_r\left(\cos\theta\cos\theta_s - \sin\theta\sin\phi\sin\theta_s\right) \\ & -2H_\theta\left(\sin\theta\cos\theta_s + \cos\theta\sin\phi\sin\theta_s\right)\Big\}\Big|_{y=-d}\end{aligned} \tag{21}$$

and

$$\begin{aligned}-J_z = \Big\{ & 2H_r\left[\sin\theta\left(\cos\phi_s\cos\phi - \sin\phi_s\cos\theta_s\sin\phi\right) - \cos\theta\sin\phi_s\sin\theta_s\right] \\ & + 2H_\theta\left[\cos\theta\left(\cos\phi_s\cos\phi - \sin\phi_s\cos\theta_s\sin\phi\right) + \sin\theta\sin\phi_s\sin\theta_s\right]\Big\}\end{aligned} \tag{22}$$

where

$$\sin \phi = y'/\left(x'^2 + y'^2\right)^{1/2} \tag{23}$$

$$\cos \phi = x'/\left(x'^2 + y'^2\right)^{1/2} \tag{24}$$

supplement the earlier results (11) through (13).

Figure 6 gives sample calculations for a dipole oriented normal to a conducting plane. Because of the rotational symmetry, the current density is plotted in terms of the cylindrical component J_ϕ rather than the rectangular components given in (21) and (22). The plot is normalized with respect to a reference surface current magnitude as shown on the ordinate axis. The parameter for the various curves is the distance of the dipole from the plane in tenths of one skin depth. It is to be observed from figure 6 that, even with increasing separation in the ocean between source and conducting plate, where the electrical parameters have been taken to be $\epsilon_r = 80$, $\sigma = 4$, the region of influence does not extend significantly beyond a region given by a circular area of one skin depth in radius centered at the point on the plane nearest the dipole.

MODIFICATION OF THE INDUCED CURRENT DISTRIBUTION ON VERTICAL INFINITE CONDUCTING PLATE DUE TO THE PRESENCE OF AIR-OCEAN INTERFACE: MAGNETIC DIPOLE EXCITATION

Approximate boundary conditions will be used in the sense that the conductivity of the conducting plate will be assumed infinite ($\underline{n} \times \underline{E} = 0$, $\underline{n} \cdot \underline{H} = 0$) while at the air-ocean interface the dielectric discontinuity is assumed sufficiently large so that the approximation, $\underline{n} \times \underline{H} = 0$, $\underline{n} \cdot \underline{E} = 0$ can be used. In terms of reflection coefficients this means that at the plate $\rho = +1$ while at the air-ocean interface $\rho = -1$. Under this approximation, the image theory can again be used to yield a solution in a direct manner. It is to be expected that the results obtained should be good unless the dipole source is very close to the air-ocean interface. The approximation at the metal plate will be excellent for any metal in common usage, provided the thickness of the metal is of the order of the characteristic skin depth in the metal. At the air-ocean interface, where at the frequencies considered here the discontinuity in the relative dielectric constant or relative permittivity is about 80, any ray incident on that interface from below will suffer total internal reflection unless the angle that the ray makes with the normal to the surface is less than approximately 6°.

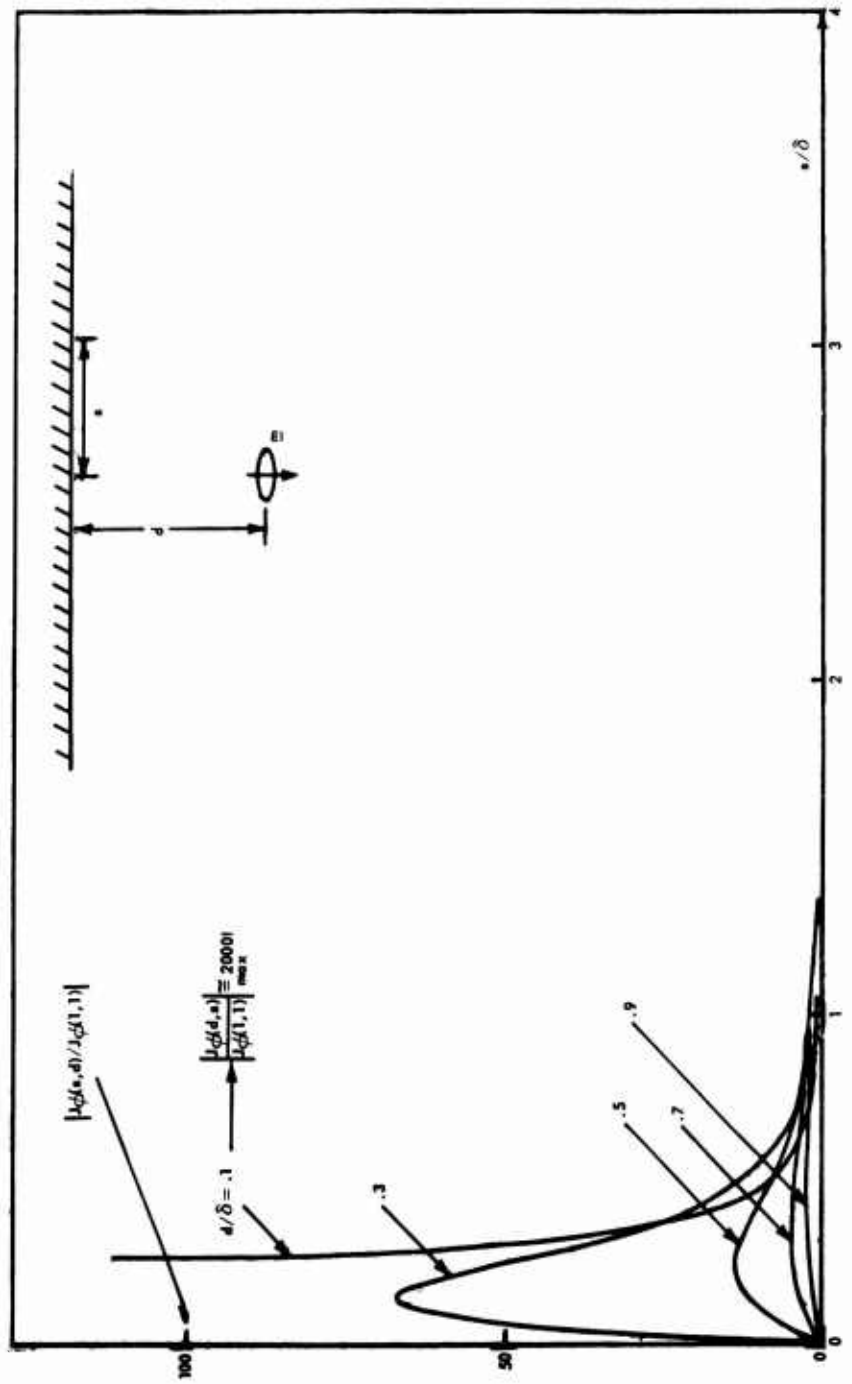

Figure 6. Surface Current Density Induced on the Plane Normalized with Respect to the Surface Current at 1 Skin Depth from Nearest Point for 1 Skin Depth Stand-off

Within this small cone, the amount of energy transmitted into the air region will be extremely small. This is due to both the small area such a cone projects upon the surface for sources within a few skin depths from the surface and the dielectric discontinuity which yields a transmission coefficient of approximately 0.2, i.e., a power transmission coefficient of 0.04. The above approximations can, therefore, be used with considerable confidence.

Figure 7 shows the image theory solution for a dipole oriented vertically. The coordinate axes of the cartesian system are oriented such that the x-y plane lies on the air-ocean interface with the origin at the conjunction of the air-ocean and metal-ocean interfaces, the y axis being placed normal to the metal surface.

The components of the total magnetic field intensity at any point in the ocean quadrant are given by

$$H_x/H_o = \sum_{i=1}^{4}\left[3(kr_i)^{-3} + 3j(kr_i)^{-2} - (kr_i)^{-1}\right] e^{-jkr_i} \sin\theta_i \cos\theta_i \cos\phi_i \quad (25)$$

$$H_y/H_o = \sum_{i=1}^{4}\left[3(kr_i)^{-3} + 3j(kr_i)^{-2} - (kr_i)^{-1}\right] e^{-jkr_i} \sin\theta_i \cos\theta_i \sin\phi_i \quad (26)$$

$$H_z/H_o = \sum_{i=1}^{4}\left\{\left[2(kr_i)^{-3} + 2j(kr_i)^{-2}\right]\cos^2\theta_i - \left[(kr_i)^{-3} + j(kr_i)^{-2} - (kr_i)^{-1}\right]\sin^2\theta_i\right\} e^{-jkr_i} \quad (27)$$

where, on the surface y = 0,

$$r_4 = r_1 \qquad \theta_4 = \theta_1 \qquad \phi_4 = 2\pi - \phi_1 = -\phi_1 \quad (28)$$

$$r_3 = r_2 \qquad \theta_3 = \theta_2 \qquad \phi_3 = 2\pi - \phi_2 = -\phi_2 = -\phi_1 . \quad (29)$$

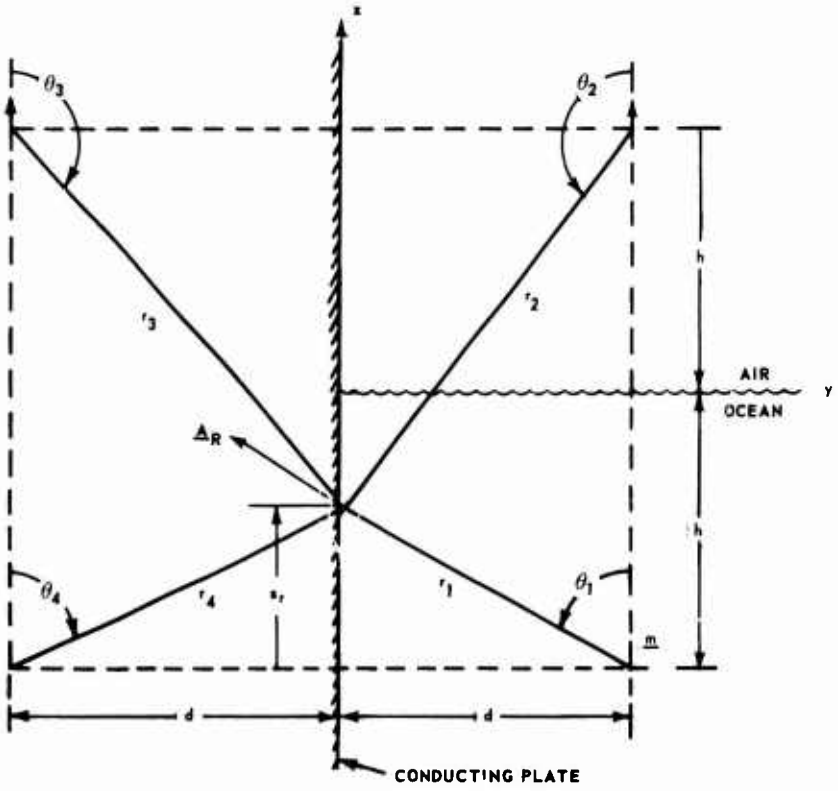

Figure 7. Image Theory Applied to Modified Geometry

On this surface, the induced surface current is given by

$$\begin{aligned}\underline{J} &= \underline{n} \times \underline{H} \\ &= \underline{a}_y \times \left[H_x \underline{a}_x - H_z \underline{a}_z\right] \\ &= H_z \underline{a}_x - H_x \underline{a}_z \ . \end{aligned} \tag{30}$$

Therefore,

$$\begin{aligned} J_x/H_o &= H_z/H_o \\ J_z/H_o &= -H_x/H_o \end{aligned} \tag{31}$$

where, consequently,

$$J_x/H_o = 2\sum_{i=1}^{2} \left\{2\left[(kr_i)^{-3} + j(kr_i)^{-2}\right]\cos^2\theta_i - \left[(kr_i)^{-3} + j(kr_i)^{-2} - (kr_i)^{-1}\right]\sin^2\theta_i\right\} e^{-jkr_i} \tag{32}$$

and

$$J_z/H_o = -2\sum_{i=1}^{2}\left[3(kr_i)^{-3} + 3j(kr_i)^{-2} - (kr_i)^{-1}\right] e^{-jkr_i} \sin\theta_i \cos\theta_i \cos\phi_1 \tag{33}$$

where

$$r_1^2 = x^2 + d^2 + (z + h)^2 \tag{34}$$

$$\sin\theta_1 = \left(x^2 + d^2\right)^{1/2}/r_1 \tag{35}$$

$$\cos\theta_1 = (z + h)/r_1 \tag{36}$$

$$\cos\phi_1 = x/\left(d^2 + x^2\right)^{1/2} \tag{37}$$

$$r_2^2 = x^2 + d^2 + (h - z)^2 \tag{38}$$

$$\sin\theta_2 = \left(x^2 + d^2\right)^{1/2}/r_2 \tag{39}$$

$$\cos\theta_2 = (z - h)/r_2 \ . \tag{40}$$

Two other orientations, orthogonal to the first, are possible and may be of interest. These and their corresponding image theory solutions are shown in figures 8 and 9. Expressions corresponding to equations (32) through (40) are readily obtained. Thus, the results for an arbitrarily oriented dipole may be obtained through suitable superposition of these cases. If the dipole in figure 7 were oriented at angles (θ_m, ϕ_m) with respect to the cartesian coordinate system,

$$m_z = m \cos \theta_m \tag{41}$$

$$m_y = m \sin \theta_m \sin \phi_m \tag{42}$$

$$m_x = m \sin \theta_m \cos \phi_m \tag{43}$$

is obtained, where m_z, m_y, and m_x are the dipole moments to be inserted in the expressions corresponding to the cases shown in figures 7, 8, and 9, respectively.

It should be emphasized that the solution obtained holds only for the region $y > 0, z < 0$ (the ocean) and cannot be extended successfully beyond that region. Thus, the surface current induced on the metallic plane can only be obtained for the submerged part. As indicated earlier in this section, little energy penetrates into the air region and, therefore, the induced currents above the line $z = 0, y = 0$ will have little or no effect on the final result. The only exception to this would occur if the dipole were located close to the coordinate origin, where it would be in the immediate proximity of the conducting plane and only just under the surface. In this case substantial errors might well result.

THE INFLUENCE OF THE AIR-OCEAN INTERFACE ON A DETECTOR ORIENTED ORTHOGONAL TO, AND AT A DISTANCE b FROM, THE SOURCE

The results of the previous section were extended to allow an examination of changes in signal detection due to the presence of the air-ocean interface when the source-detector system approached the infinite conducting plate. To this end, equations (25) through (27) become pertinent for the case corresponding to figure 7 where the dipole source is located at the point $x = 0, y = d$, $z = -h$, and the detector is located at the point $x = b \cos \phi_b$, $y = d + b \sin \phi_b$, $z = -h$; i.e., the detector is presumed to be located in the same horizontal plane as the source and separated from it by a distance b. The direction of b makes an angle of ϕ_b with the $y = 0$ plane.

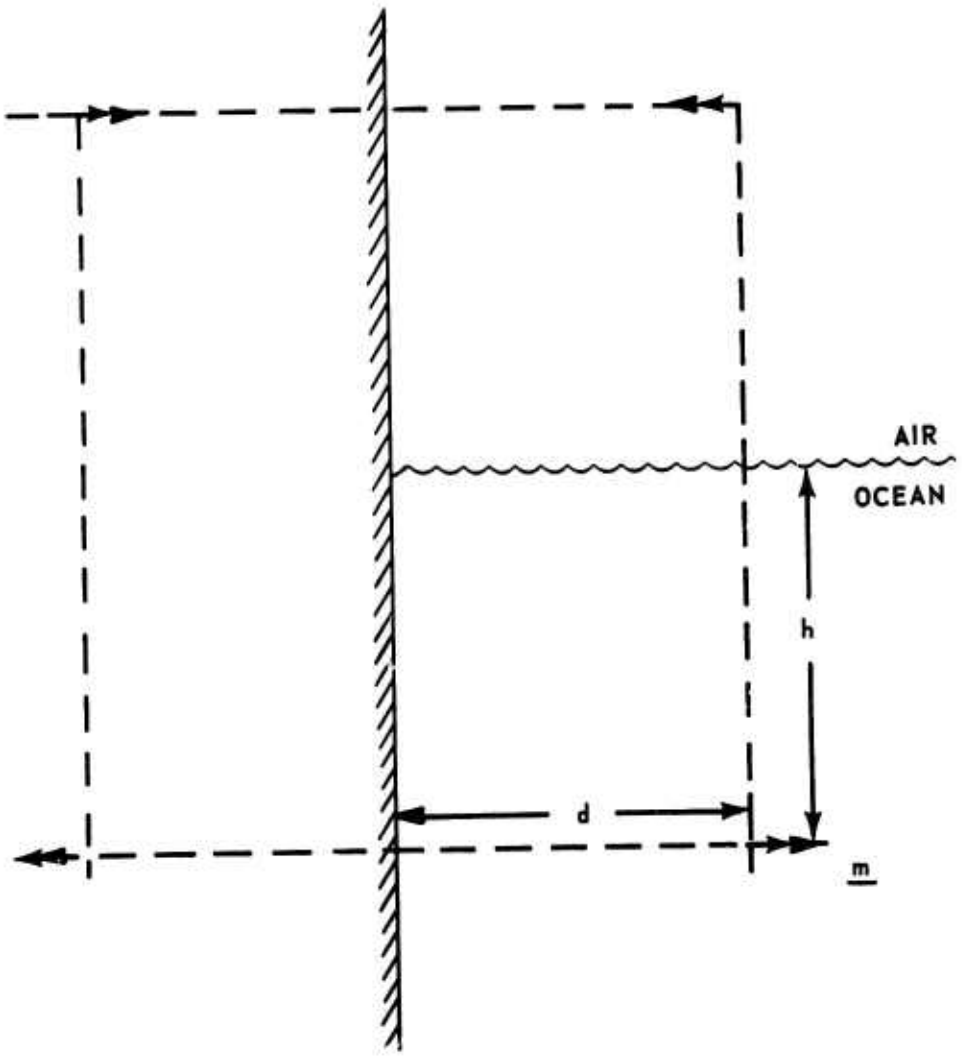

Figure 8. Dipole Source Normal to Conducting Plane

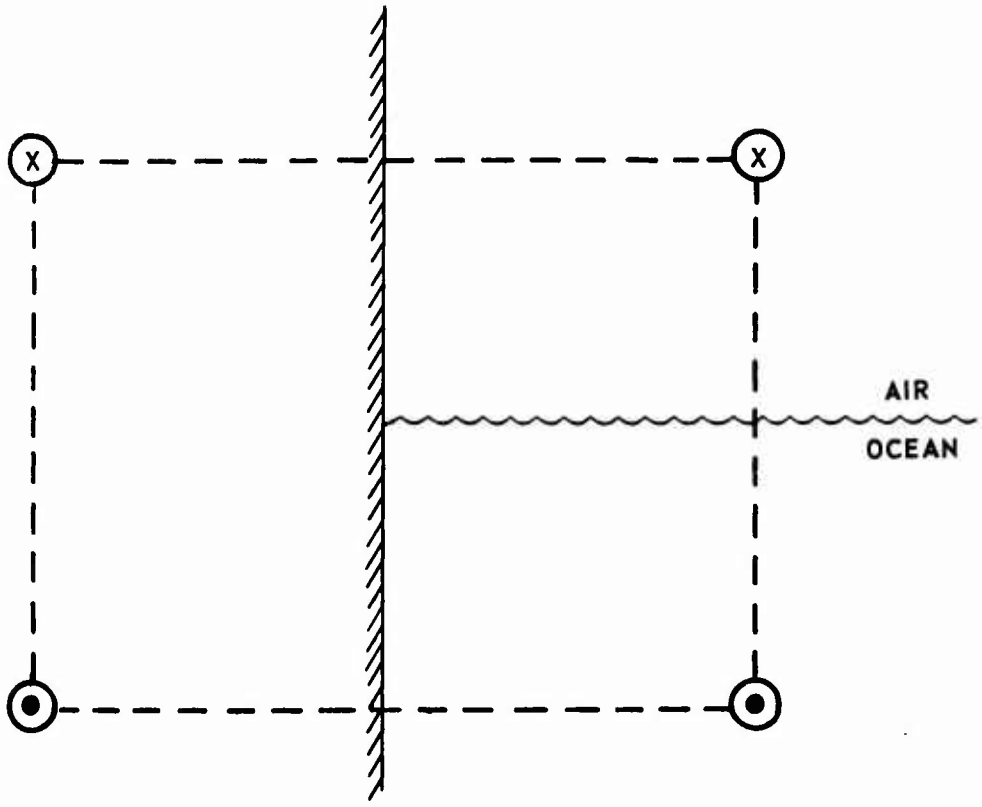

Figure 9. Dipole Source Parallel to Both Air-Ocean and Air-Metal Interfaces

The expressions for (r_i, θ_i, ϕ_i) become, for a general detector location (x_d, y_d, z_d),

$$r_1^2 = x_d^2 + (y_d - d)^2 + (z_d + h)^2 \tag{44}$$

$$r_2^2 = x_d^2 + (y_d - d)^2 + (z_d - h)^2 \tag{45}$$

$$r_3^2 = x_d^2 + (y_d + d)^2 + (z_d - h)^2 \tag{46}$$

$$r_4^2 = x_d^2 + (y_d + d)^2 + (z_d + h)^2 \tag{47}$$

$$\sin \theta_1 = \left[x_d^2 + (y_d - d)^2\right]^{1/2}/r_1, \quad \cos \theta_1 = (z_d + h)/r_1 \tag{48}$$

$$\sin \theta_2 = \left[x_d^2 + (y_d - d)^2\right]^{1/2}/r_2, \quad \cos \theta_2 = (z_d - h)/r_2 \tag{49}$$

$$\sin \theta_3 = \left[x_d^2 + (y_d + d)^2\right]^{1/2}/r_3, \quad \cos \theta_3 = (z_d - h)/r_3 \tag{50}$$

$$\sin \theta_4 = \left[x_d^2 + (y_d + d)^2\right]^{1/2}/r_4, \quad \cos \theta_4 = (z_d + h)/r_4 \tag{51}$$

and

$$\sin \phi_1 = (y_d - d)/\left[x_d^2 + (y_d - d)^2\right]^{1/2}, \quad \cos \phi_1 = x_d/\left[x_d^2 + (y_d - d)^2\right]^{1/2} \tag{52}$$

$$\phi_2 = \phi_1 \tag{53}$$

$$\sin \phi_3 = (y_d + d)/\left[x_d^2 + (y_d + d)^2\right]^{1/2}, \quad \cos \phi_3 = x_d/\left[x_d^2 + (y_d + d)^2\right]^{1/2} \tag{54}$$

$$\phi_4 = \phi_3 . \tag{55}$$

If, as previously mentioned, the detector location is constrained to the horizontal plane containing the source, then the component of the magnetic field intensity which is of particular interest is the one lying in the direction of the baselength b,

$$H_b = H_x \cos \phi_b + H_y \sin \phi_b ,$$

since in the absence of the metallic plane and the air-ocean interface this component will vanish. The vertical component at the detector is

$$H_v = H_z$$

and the component normal to both H_b and H_o is

$$H_n = H_y \cos \phi_b - H_x \sin \phi_b .$$

Figures 10, 11, and 12 give the results of some of the calculations performed on this system. The ordinates represent the EMF induced in a coil of radius a located in a plane normal to the baseline b at the detector location. The EMF is normalized with respect to the EMF induced in the same coil when located with its axis coincident with the source in a plane normal to the magnetic dipole, and is expressed in dB's. All linear quantities are normalized with respect to the electromagnetic skin depth in the ocean. The variation in the signal level is shown as the dipole source approaches the conducting plane at various constant depths from 0.1 to 1.5 skin depths. The effect of the detector orientation with respect to the conducting plane is shown in some sample cases.

It is evident that the effect of the air-ocean interface is strong and masks the effect of the conducting plane at shallow depths until the dipole has approached to within one-half skin depth. At greater depths, one skin depth or more, the infinite conducting plane is first "seen" at about two skin depths. The three figures correspond to baselengths of 0.075, 0.150, and 0.250, successively, and indicate that decreasing the baselength increases the rate at which the signal changes once the conducting plane has been "seen."

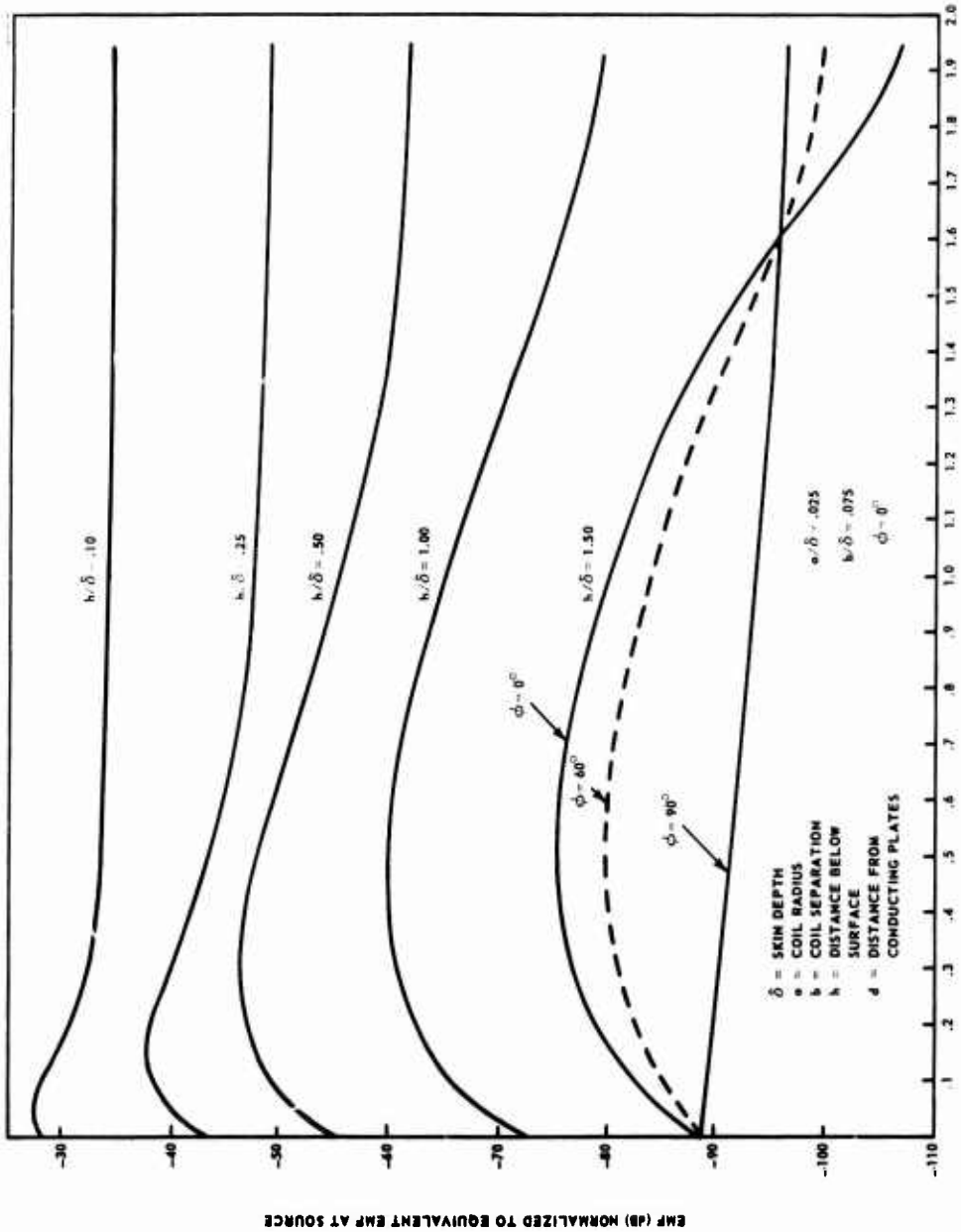

Figure 10. EMF Induced in Orthogonal Detector as a Function of Depth and Stand-off: Baselength 0.075 δ

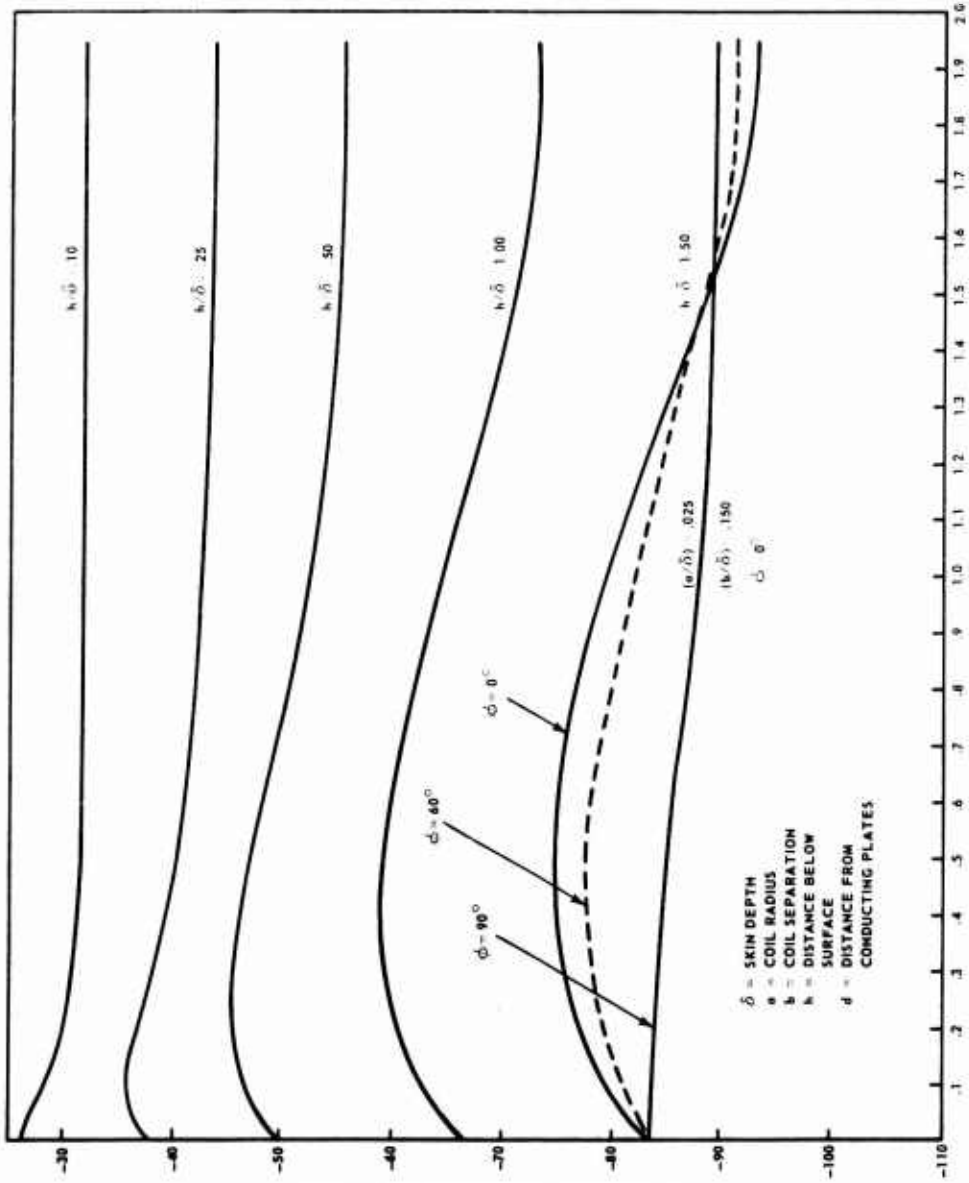

Figure 11. EMF Induced in Orthogonal Detector as a Function of Depth and Stand-off: Baselength 0.150 δ

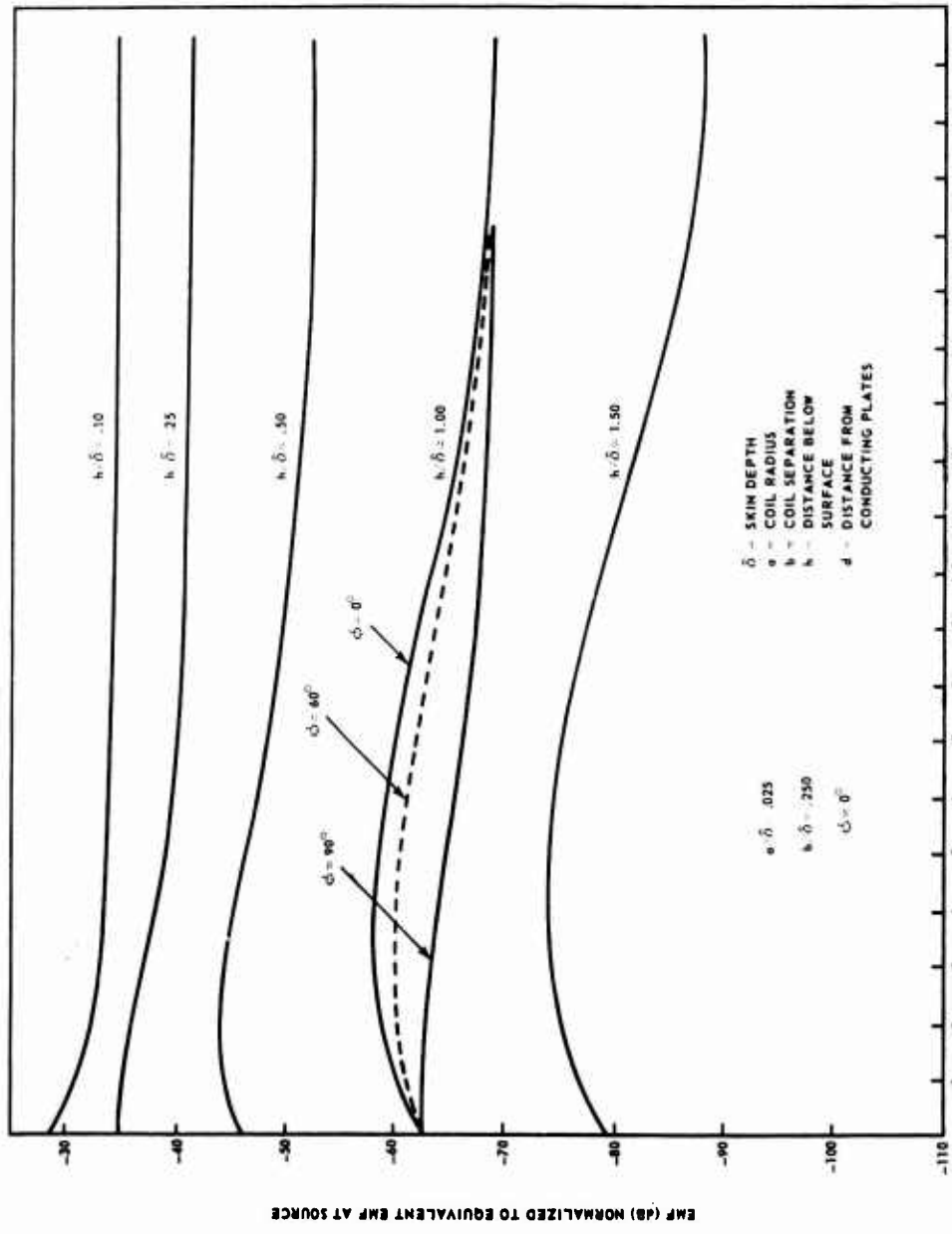

Figure 12. EMF Induced in Orthogonal Detector as a Function of Depth and Stand-off: Baselength 0.250 δ

SUMMARY

This report consists of three parts. The surface current distribution induced by a magnetic dipole on an infinite conducting plane was investigated when both were immersed in a lossy medium, the ocean. It was found that the surface current distribution did not extend materially beyond a circular area of about one skin depth in radius centered on the point on the conducting plane nearest the dipole source. This result was then generalized to include the case where the effect of an air-ocean interface was included. In the third and final part, the signal induced in a detector coil was obtained for a vertical magnetic dipole in the ocean in the presence of an infinite vertical perfectly conducting plane and a horizontal air-ocean interface. The spacing between the detector and source was varied in the same horizontal plane, while the detector coil was oriented orthogonally to the magnetic dipole and its axis was in line with the baselength. It was found that the air-ocean interface affected the signal severely and masked the presence of the conducting plane for shallow-depth runs. At greater depths, as expected, the air-ocean interface effect is rapidly lost. Appendixes A and B contain the computer programs used for computations pertaining to the first and third parts of this report.

REVERSE BLANK

Appendix A

CURRENT DISTRIBUTION ON AN INFINITE PLATE AS A FUNCTION OF MAGNETIC DIPOLE DEPTH FROM THE PLATE

```
C       CURRENT DISTRIBUTION J SUB PHI ON AN INFINITE PLATE AS A
C       FUNCTION OF MAGNETIC DIPOLE DEPTH FROM PLATE. S EQUALS
C       S OVER DELTA, D EQUALS D OVER DELTA WHERE DELTA IS THE
C       SKIN DEPTH, D IS A MEASURE OF THE DIPOLE DEPTH, S IS A MEAS-
C       URE OF THE DISTANCE FROM THE POINT ON THE PLATE DIRECTLY
C       ABOVE THE DIPOLE.
      READ 1, DMIN, DMAX, DD, SMAX, DS
    1 FORMAT(5F10.4)
      D=DMIN
    3 S=0.
      DENOM=(((1.+(2.**.5))**2+((4.-(2.**.5))**2))**.5
    2 RATIO=S*D/((S*S+D*D))**2.5)
      SUM=(S*S+D*D)**.5
      TOP=((1.+SUM)**2+(2.*SUM*SUM-SUM)**2)**.5
      EX=-SUM
      FF=EXPF(EX)
      TOTAL=4.*(2.**.5)*RATIO*FF*TOP/DENOM
      PRINT 4, D, S, TOTAL
    4 FORMAT(5H D = ,E10.4,5H S = ,E10.4,14H  J SUB PHI = ,E15.8)
      S=S+DS
      IF(S-SMAX)2,2,5
    5 D=D+DD
      IF(D-DMAX)3,3,6
    6 END
```

Note: The current distribution has been normalized such that the output is in the form $J_{\phi}(d,s)/J_{\phi}(\delta,\delta)$.

Appendix B

SIGNAL INDUCED IN A DETECTOR COIL AS A FUNCTION OF THE SUBMERGED DISTANCE FROM AN INFINITE CONDUCTING VERTICAL PLATE

```
C     SIGNAL INDUCED IN DETECTOR COIL AS A FUNCTION OF SUB-
C     MERGED DEPTH. DISTANCE FROM AN INFINITE CONDUCTING
C     VERTICAL PLATE. BASE LENGTH AND ANGLE OF BASE LENGTH
C     TO VERTICAL FROM THE INFINITE PLATE TO THE DIPOLE ELE-
C     MENT. DIPOLE ORIENTATION IS VERTICAL AND THE NORMAL TO
C     THE DETECTOR COIL LIES IN THE HORIZONTAL PLANE. FURTHER
C     PARAMETERS ARE -A THE COIL RADIUS, N1 NUMBER OF TURNS
C     ON PRIMARY COIL, N2 NUMBER OF TURNS ON THE DETECTOR
C     COIL. ALL LINEAR DIMENSIONS ARE NORMALIZED W.R.T. THE
C     SKIN DEPTH IN SEA WATER. PHI IS TO BE ENTERED IN DEGREES.
      REAL N1,N2
      DIMENSION HH(10),BB(10),BPHI(10)
      HH(1)=.1
      HH(2)=.25
      HH(3)=.50
      HH(4)=1.00
      HH(5)=1.50
      BB(1)=.075
      BB(2)=.150
      BB(3)=.250
      BPHI(1)=0.
      BPHI(2)=30.
      BPHI(3)=60.
      BPHI(4)=90.
      DMAX=2.000
      A=.025
      N1=1.
      N2=1.
      DO 6 I=1,5,1
      H=HH(I)
      DO 8 J=1,3,1
      B=BB(J)
      DO 7 K=1,4,1
      BHI=BPHI(K)
      PRINT 2,DMAX,H,B,BHI,A,N1,N2
```

```
    2 FORMAT(7H DMAX= E10.3,4H H= E10.3,4H B= E10.3,6H
     1PHI= E10.3,4H A= E10.3,5H N1= E10.3,5H N2= E10.3)
      PRINT 3
    3 FORMAT(40H     D      EMF      EMFDB)
      BHI=(BHI/180.)*3.1415927
      DO 9 M=1,40
      D=.05*(M-1)
      R3=(4.*H*H+B*B)**.5
      R4=(R3*R3+4.*D*D+4.*D*B*COSF(BHI))**.5
      CS3=2.*H/R3
      SI3=B/R3
      CS4=2.*H/R4
      SI4=(4.*D*D+B*B+4.*D*B*COSF(BHI))**.5/R4
     BHI4=ATANF(B*SINF(BHI)/(2.*D+B*COSF(BHI)))
      DENOM=(-A*COSF(A)+(1.+A)*SINF(A))*EXPF(-A)/(A*A)
      T3=A/(R3*R3*R3)
     T4=A/(R4*R4*R4)
     S3=(1.+R3)*SINF(R3)
     S4=(1.+R4)*SINF(R4)
     TOP1=T3*(-R3*COSF(R3)+S3)*EXPF(-R3)*CS3
     TOP2=(T3/2.)*(-R3*(1.+2.*R3)*COSF(R3)+S3)*EXPF(-R3)*SI3
     TOP3=T4*(-R4*COSF(R4)+S4)*EXPF(-R4)*CS4
     TOP4=(T4/2.)*(-R4*(1.+2.*R4)*COSF(R4)+S4)*EXPF(-R4)*SI4
     CS5=COSF(BHI-BHI4)
     TOP=TOP1*S13+TOP2*CS3+TOP3*SI4*CS5+TOP4*CS4*CS5
     EMF=TOP/DENOM
     EMF=ABSF(EMF)
     EMFDB=20.*ALOG(EMF)/2.302585
     PRINT 4,D,EMF,EMFDB
   4 FORMAT(3E15.5)
   9 CONTINUE
   7 CONTINUE
   8 CONTINUE
   6 CONTINUE
     END
```

DISTRIBUTION LIST

Addressee	No. of Copies
Chief of Naval Operations (NOP-03EG)	2
Naval Ordnance Systems Command (ORD-0632) For dissemination within NOSC as follows: ORD-035; ORD-05121; ORD-541; ORD-5413; ORD-0632 (2 copies).	6
DDC, Alexandria, Va.	2
NTS, Keyport (QEEL Technical Library)	1
NOL, White Oak	2
ARL, Penn State (Attn: Dr. Piggot)	1
APL, U/W Seattle	1

UNCLASSIFIED
Security Classification

DOCUMENT CONTROL DATA - R & D

Security classification of title, body of abstract and indexing annotation must be entered when the overall report is classified)

1. ORIGINATING ACTIVITY (*Corporate author*)

Naval Underwater Systems Center
Newport, Rhode Island 02840

2a. REPORT SECURITY CLASSIFICATION

UNCLASSIFIED

2b. GROUP

3. REPORT TITLE

Electromagnetic Surface Currents Induced By A Magnetic Dipole Source on Infinite Perfectly Conducting Surfaces In the Presence of an Air-Ocean Interface

4. DESCRIPTIVE NOTES (*Type of report and inclusive dates*)

5. AUTHOR(S) (*First name, middle initial, last name*)

Donald M. Bolle

6. REPORT DATE	7a. TOTAL NO. OF PAGES	7b. NO. OF REFS
11 April 1973	34	none

8a. CONTRACT OR GRANT NO	9a. ORIGINATOR'S REPORT NUMBER(S)
b. PROJECT NO	TR 4322
c. ORD-541-451/091-1/UF17-351-501	9b. OTHER REPORT NO(S) (*Any other numbers that may be assigned this report*)
d.	

10. DISTRIBUTION STATEMENT

Distribution limited to U. S. Government agencies only; test and evaluation; 11 April 1973 Other requests for this document must be referred to the Naval Underwater Systems Center, Newport, Rhode Island 02840.

11. SUPPLEMENTARY NOTES	12. SPONSORING MILITARY ACTIVITY
	NOSC

13. ABSTRACT

The electromagnetic surface currents induced by a magnetic dipole on infinite perfectly conducting surfaces in the presence of a sea-air interface, as well as in a homogeneous ocean environment, are obtained. The method used is that of images where the approximation of a -1 reflection coefficient at the sea-air interface may be justified and used. Computer programs and results which yield a clear insight into the sphere of influence of the magnetic dipole in such an environment when displayed graphically are given.

DD FORM 1 NOV 65 1473 (PAGE 1)

UNCLASSIFIED
Security Classification

14 KEY WORDS	LINK A		LINK B		LINK C	
	ROLE	WT	ROLE	WT	ROLE	WT
electromagnetic surface currents air-ocean interfaces magnetic dipole						